Visualization and Characterization of Colloidal Growth from Ramified to Faceted Structures

A. T. Skjeltorp
Institute for Energy Technology, N-2007 Kjeller, Norway
(Received 8 September 1986)

Uniformly sized microspheres confined to thin layers between solid boundaries are used to demonstrate pattern formation in diffusion-controlled aggregation. Extremely slow growth processes monitored over several months show faceted hexagonal lattices. For successively faster growth, dendritic crystals and ramified aggregates are formed. The results are compared with recent studies of local and global growth models.

PACS numbers: 64.60.Cn, 05.40.+j, 68.70.+w, 82.70.Dd

The formation of aggregates, dendrites, and crystals from small subunits like atoms and colloidal particles occurs in a wide range of phenomena in science and technology. The models used to describe these processes have aimed at reproducing the characteristic patterns of the resulting structures following essentially two approaches. One is the simple diffusion-limited-aggregation (DLA) computer-simulation model initiated by Witten and Sander.[1] Here, randomly diffusing particles are made to stick irreversibly to the growing aggregate. These computer experiments produce irregular ramified objects which have been characterized by a Hausdorff fractal dimension D less than the Euclidean dimension d.

The other approach relates to modeling of the dendritic crystal growth and tip splitting found in undercooled melts as studied extensively by Langer and others.[2] At present there is no direct relationship found between fractal aggregation and dendritic crystal growth, neither analytically nor experimentally. However, extensive computer simulations have been made to establish possible universality classes, crossover from nonequilibrium to equilibrium behavior, and the appearance of dendritic clusters.[3] Certain aspects of these problems have thus been probed in various modifications of the initial Witten-Sander DLA model believed to be closer to physical realizations. These include diffusion-limited cluster aggregation (DLCA),[4,5] cluster rotations,[5] lattice effects,[6] disaggregation,[7] surface tension,[8,9] and wedge formation.[10]

However, it remains to be seen how accurately these deterministic computer codes reflect nature, as the number of experiments on real systems allowing direct observations are very few compared to the number of simulations. As most simulations are carried out in two dimensions (2D),[3] experimental realizations in 2D systems are particularly important.

The purpose of this paper is to report first experiments that use prototypical colloidal particles to visualize a wide range of these processes (see Fig. 1). It has thus been possible to demonstrate the time scale involved in going from nonequilibrium to a true equilibrium situation, and to find quantitative growth conditions producing aggregates of fractal clusters, compact clusters with rough surfaces, dendritic or snowflakelike patterns, and compact faceted crystals. In addition, this paper also reports the first 2D DLCA experiments which may be compared directly with recent simulations, allowing structural readjustments[5] besides particle and cluster-cluster aggregation.[4] Compared to recent DLA studies of zinc electrodeposits in a plane,[11] the present use of colloidal particles provides a new level of detailed observations to gain insight into the controlling parameters for a wider range of growth morphologies.

So far, it appears that there has been only one report of a physical realization of diffusion-controlled aggregation of microparticles in a plane.[12,13] This involved the use of 0.3-μm-diam silica spheres on a water-air interface producing aggregates with fractal dimensions $D=1.20\pm0.15$. This value is well below the simulated value $D\simeq1.44$ for DLCA,[5] and attributed to anisotropic electrostatic forces around the growing tips. Other experiments on particles which have not been diffusion controlled have shown aggregation induced by convection,[14] shear,[15] ac electric fields,[16] and ac magnetic fields in ferrofluid.[17] Curiously enough, these processes have produced aggregates with fractal dimensions $D\simeq1.7$, close to the simulated DLA value and thus significantly higher than the DLCA value $D\simeq1.44$.

The present experimental system consisted of very uniformly sized polystyrene spheres[18] with diameters $a=1.1$ and 4.7 μm dispersed in water and confined to essentially one layer between two prepared glass plates. The separation between the plates could be adjusted evenly by use of a small fraction of larger spheres as spacers. An inverted microscope with video-camera attachment allowed direct long-term observations and digital analysis of the structure with use of a frame grabber with 512×512-pixel resolution.

The spheres were stabilized with a surfactant (0.1% sodium dodecyl sulphate) and ionic strength of 0.02 mol. The Derjaguin-Landau-Verwey-Overbeck model[19] shows that for this case the interaction potential for two spheres will have a "secondary minimum" (attractive forces) of approximately $0.3kT$ and $4kT$ for the 1.1-μm and 4.7-μm spheres, respectively. This indicates that the 1.1-μm spheres will need roughly three or more neigh-

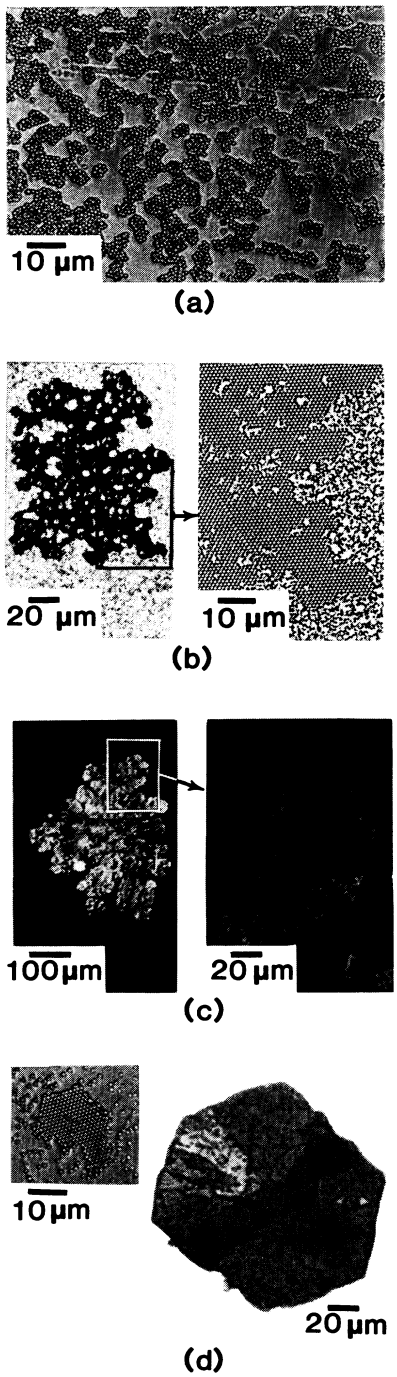

FIG. 1. Microscope pictures of aggregated 1.1-μm spheres for various average growth periods (t), initial concentration (ρ), and average growth velocity (v_g) as discussed in the text: (a) ramified clusters ($t=20$ min, $\rho\simeq 0.3$, $v_g\simeq 2\times 10^{-2}$ μm/sec), (b) "porous" cluster with rough surface ($t=100$ h, $\rho\simeq 0.7$, $v_g\simeq 3\times 10^{-4}$ μm/sec), (c) dendritic crystal ($t\simeq 4000$ h, $\rho\simeq 0.15$, $v_g\simeq 10^{-5}$ μm/sec) at two different magnifications, (d) faceted hexagonal crystal ($t\simeq 4500$ h, $\rho\simeq 0.1$, $v_g\simeq 5\times 10^{-6}$ μm/sec) with small seed crystal shown in the left inset.

bors to obtain a total bonding energy $\geq kT$ to overcome the disrupting Brownian motion, whereas the 4.7-μm spheres will readily aggregate. In one case [Fig. 1(a)], salt was added (0.05 mol) to the 1.1-μm dispersion to reduce the Coulomb repulsion and produce strong van der Waals bonding.

Figure 1 displays a series of growth patterns for samples containing typically 10^7–10^8 1.1-μm dispersed spheres. Figure 1(a) shows the usual DLCA situation with relatively fast irreversible clustering for a sphere concentration $\rho\simeq 0.30$ defined relative to a compact lattice (for which $\rho=1$). A quantitative analysis of this case will be presented later in this paper. Figures 1(b)–1(d) show examples of successively slower DLA growth. Here, the growing clusters were thus so far apart that only single spheres stuck to the aggregates and there was no clustering of clusters.

Figure 1(b) shows a snapshot of a slowly growing aggregate 100 h after initiation of the growth process with an average growth velocity of $v_g\simeq 3\times 10^{-4}$ μm/sec (defined as the average growth of radius of gyration from the initiation) and with a fairly high particle density $\rho\simeq 0.7$. The particle diffusion was thus very inhibited and the perimeter of the growing crystal was "bombarded" rather uniformly by the spheres, but with a low sticking probability. This situation is believed to be close to the physical realization of growth according to an Eden[20] or Rikvold[8] model. In the Eden model particles are added at random sites at the perimeter of the growing aggregate. The Rikvold model[8] contains the added features of surface tension and the effects of a screening length l_D proportional to the diffusion constant in the medium. Considering the square lattice used in Rikvold's simulations, the cluster in Fig. 1(b) shows a striking resemblance to the cluster in Fig. 3 of his paper[8] with a screening length of $l_D=4$ lattice constants. The irregularity of the surface has been analyzed and discussed elsewhere[21] and compared with recent scaling results from simulations.[20]

Figure 1(c) shows a situation of dendritic growth with an average growth velocity of approximately $v_g=10^{-5}$ μm/sec during five months. The starting concentration in this case was relatively low ($\rho\simeq 0.15$). The overall pattern is "snowflakelike" with branching dendrites as shown in the magnified picture.

Finally, Fig. 1(d) shows a nearly perfect hexagonal single crystal (some dislocations) which has grown for a period of about six months from an initial concentration of $\rho\simeq 0.1$. The growth velocity here was so low ($v_g\simeq 5\times 10^{-6}$ μm/sec) that a completely equilibrium situation was achieved. Observations during growth showed that there was an even, slow layer-by-layer faceted growth from the seed crystal shown in the left inset.

It is possible to obtain a quantitative characterization of isolated clusters, exemplified by Figs. 1(b)–1(d), based on the determination of a bulk and perimeter fractal dimension, D_b and D_p, respectively, versus growth ve-

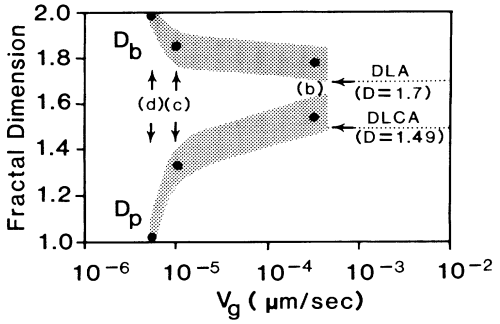

FIG. 2. Bulk (D_b) and perimeter (D_p) fractal dimensions vs growth velocity, v_g, for DLA of 1.1-μm spheres. The bands reflect the uncertainties in the determination of D_b and D_p for a wide range of clusters. Points labeled b–d correspond to the photographs in Fig. 1. Also marked in the figure is the bulk simulated value for DLA and the DLCA value obtained in the present work (Fig. 4).

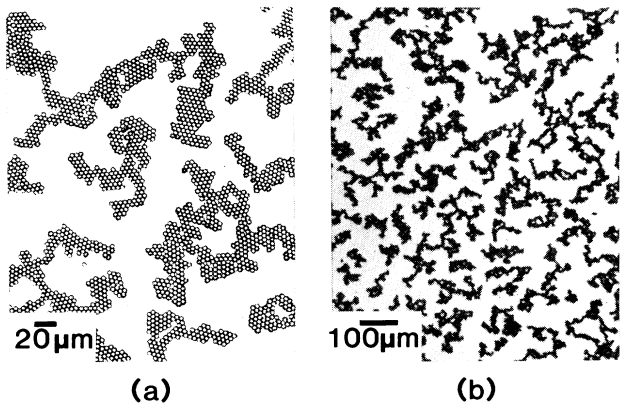

FIG. 3. DLCA of 4.7-μm spheres ($\rho=0.14$) showing (a) crystalline behavior on short length scales and (b) ramified clusters on large length scales.

locity. For this, D_b was determined in the usual way[3] from the relationship between the total number of particles N in the cluster and the radius of gyration R_g;

$$N \propto R_g^{D_b}. \tag{1}$$

Here, R_g was calculated with use of

$$R_g^2 = N^{-1} \sum_{i=1}^{N} (\mathbf{r}_i - \mathbf{r}_0)^2, \tag{2}$$

with $\mathbf{r}_0$ the center of mass for the cluster and the sum taken over all particles N positioned at sites $\mathbf{r}_i$. The log-log plot of N vs R_g at successive stages of growth thus has slope D_b. The perimeter fractal dimension D_p was obtained by use of the box-counting technique.[3] The number of $L \times L$ square boxes $N_{\text{box}}(L)$ needed to cover the perimeter was counted and averaged over different center points. For a fractal structure it is expected that

$$N_{\text{box}}(L) \propto L^{-D_p}, \tag{3}$$

and D_p may be determined from a log-log plot of $N_{\text{box}}(L)$ vs L.

On the basis of approximately one hundred growth patterns, exemplified by Fig. 1, Fig. 2 shows the phase diagram of DLA for 1.1-μm spheres expressed as D_b and D_p versus growth velocity v_g. The bands in the figure reflect the uncertainties involved in the determination of the fractal dimension. It may be seen that both D_b and D_p appear to approach the simulated DLA value 1.7 for the fastest growth in the present experiments. As v_g decreases, there is a crossover to the compact values $D_b = 2$ and $D_p = 1$ as expected for single-crystal growth.

The final portion of this paper will analyze in detail a prototypical DLCA process believed to be very close to a physical realization of the recent computer simulations by Meakin and Jullien (MJ).[5] Their model allows for cluster-cluster aggregation as well as cluster rotations around points of contact. For these experiments 4.7-μm spheres were used. The clustering was slow because of small Brownian motion but irreversible because of the secondary potential minimum discussed earlier. Figure 3 shows the aggregates formed after 24 h from an initial concentration of dispersed spheres of $\rho=0.14$. Direct observations during the growth process showed that the spheres stuck fairly close to where they came in close contact with the aggregate. There was a tendency for some rearrangement of the spheres by migration from the first nearest-neighbor site reached to an energetically more favorable neighbor site. During the clustering-of-clusters process, there was also a rotation of clusters around the point of contact. The rotations predominantly went in the direction of the smallest angle to make closed loops with a second point of contact for the clus-

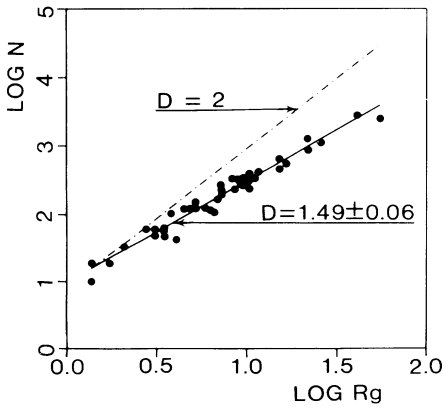

FIG. 4. Determination of fractal dimension D for DLCA clusters in Fig. 3 by use of the radius-of-gyration method as discussed in the text. R_g is expressed in units of sphere diameter (4.7 μm).

ters. The combination of these processes thus produced crystalline behavior on small length scales as shown in Fig. 3(a), but ramified clusters on larger length scales as shown in Fig. 3(b). This is still only a tiny fraction of the total sample containing about 10^6 spheres.

The quantitative analysis of the DLA structures was carried out with use of the two methods discussed earlier to determine the fraction dimension D. In Fig. 4, the radius-of-gyration method produces a log-log plot of N vs R_g with slope $D=1.49\pm0.06$. Here, R_g is expressed in units of sphere diameter $a=4.7$ μm. An independent check of D was obtained by use of the box-counting method for which the number of boxes $N_{\rm box}(L)$ containing any part of the cluster was counted and averaged over different center points. A log-log plot of $N_{\rm box}(L)$ vs L thus produced a slope $D=1.48\pm0.05$ for box sizes $L\simeq 2$–100 sphere diameters. From these estimates I therefore conclude that $D\simeq 1.49\pm0.05$.

This result may be confronted with the MJ simulation.[5] In particular, the aggregates in Fig. 3(a) show a striking resemblance to Fig. 4 in MJ's paper. Their model in this case corresponds to the observations in the present system with cluster-cluster aggregation and rigid rotation of clusters around points of contact as discussed above. The MJ fractal dimension for this case was found to be $D=1.485\pm0.015$ by means of the radius-of-gyration method and thus very close to the value found for the present system. As noted in MJ's paper,[5] it is possible that in the limit of large clusters ($N\rightarrow\infty$), the value for D allowing for rotation could decrease to their cluster-cluster-aggregation value $D=1.438\pm0.005$ without rotations. Thus, rotations have a compacting effect on relatively small length scales but could be insignificant on large length scales. This effect and a general scaling description of the cluster size distribution[22] for the present system is discussed elsewhere.[21]

In summary, it has been possible for the first time to demonstrate colloidal growth from disordered to dendritic to faceted structures. The observations support the importance of small sticking probability or low growth velocity combined with surface-tension effects to reach the equilibrium aggregation situation. The results also support recent model simulations with an algorithm including cluster-cluster aggregation as well as cluster rotations.

The research was supported in part by Dyno Industrier A/S, the Norwegian Research Council for Science and the Humanities, and the Nansen-fund.

[1]T. A. Witten, Jr., and L. M. Sander, Phys. Rev. Lett. **47**, 1400 (1981).

[2]J. S. Langer, Rev. Mod. Phys. **52**, 1 (1980); J. Nittmann and H. E. Stanley, Nature **321**, 663 (1986).

[3]Recent reviews are found in *Scaling Phenomena in Disordered Systems,* edited by R. Pynn and A. Skjeltorp (Plenum, New York, 1985), and *On Growth and Form: Fractal and Non-Fractal Patterns in Physics,* edited by H. E. Stanley and N. Ostrowsky (Nijhoff, Hingham, MA, 1986).

[4]P. Meakin, Phys. Rev. Lett. **51**, 1119 (1983); M. Kolb, R. Botet, and R. Jullien, Phys. Rev. Lett. **51**, 1123 (1983).

[5]P. Meakin and R. Jullien, J. Phys. (Paris) **46**, 1543 (1985).

[6]L. A. Turkevich and H. Scher, Phys. Rev. Lett. **55**, 1026 (1985).

[7]R. Botet and R. Jullien, Phys. Rev. Lett. **55**, 1943 (1985).

[8]P. A. Rikvold, Phys. Rev. A **26**, 647 (1982).

[9]T. Vicsek, Phys. Rev. Lett. **53**, 2281 (1984).

[10]T. C. Halsey, P. Meakin, and I. Procaccia, Phys. Rev. Lett. **56**, 854 (1986).

[11]Y. Sawada, A. Dougherty, and J. P. Gollub, Phys. Rev. Lett. **56**, 1260 (1986); D. Grier, E. Ben-Jacob, R. Clarke, and L. M. Sander, Phys. Rev. Lett. **56**, 1264 (1986).

[12]A. J. Hurd and D. W. Schaefer, Phys. Rev. Lett. **54**, 1043 (1985).

[13]For the DLA experiments on gold colloids [see D. A. Weitz and M. Oliveria, Phys. Rev. Lett. **52**, 1433 (1984)], three-dimensional aggregates are projected onto a two-dimensional surface.

[14]C. Allain and B. Jouhier, J. Phys. (Paris), Lett. **44**, L421 (1983).

[15]C. Camoin and R. Blanc, J. Phys. (Paris), Lett. **46**, L67 (1985).

[16]P. Richetti, J. Prost, and P. Barois, J. Phys. (Paris), Lett. **45**, L1137 (1984).

[17]A. T. Skjeltorp, J. Magn. Magn. Mater. (to be published).

[18]J. Ugelstad *et al.*, Adv. Colloid Interface Sci. **13**, 101 (1980); the spheres are commercially available from Dyno Particles, P.O.B. 160, N-2001 Lillestrøm, Norway.

[19]J. M. Victor and J. P. Hansen, J. Phys. (Paris), Lett. **45**, L307 (1984).

[20]For a recent review with large-scale simulations, see P. Meakin, R. Jullien, and R. Botet, Europhys. Lett. **1**, 609 (1986).

[21]A. T. Skjeltorp, to be published.

[22]T. Vicsek and F. Family, Phys. Rev. Lett. **52**, 1669 (1984).

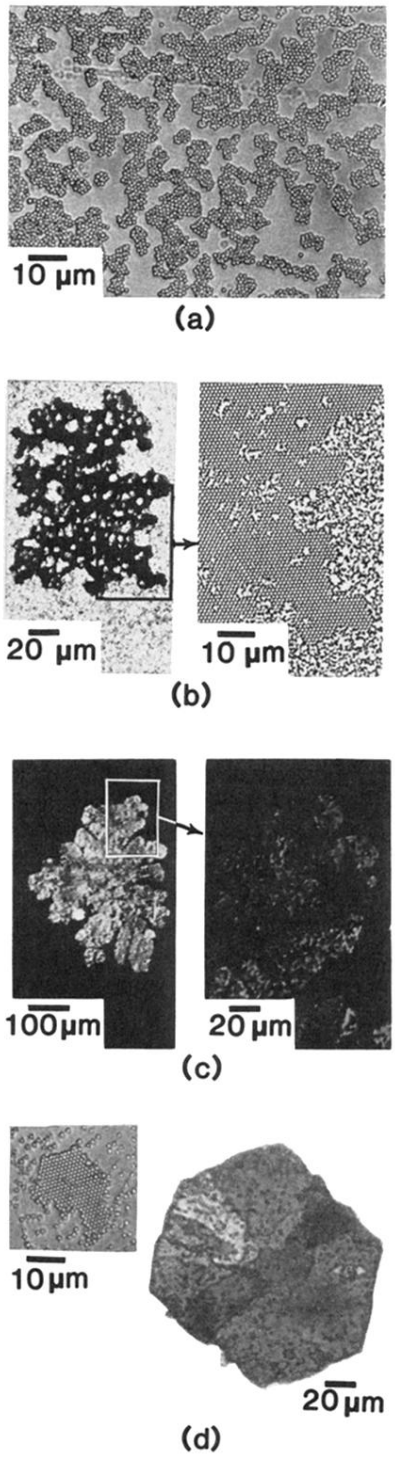

FIG. 1. Microscope pictures of aggregated 1.1-μm spheres for various average growth periods (t), initial concentration (ρ), and average growth velocity (v_g) as discussed in the text: (a) ramified clusters ($t=20$ min, $\rho\simeq 0.3$, $v_g\simeq 2\times 10^{-2}$ μm/sec), (b) "porous" cluster with rough surface ($t=100$ h, $\rho\simeq 0.7$, $v_g\simeq 3\times 10^{-4}$ μm/sec), (c) dendritic crystal ($t\simeq 4000$ h, $\rho\simeq 0.15$, $v_g\simeq 10^{-5}$ μm/sec) at two different magnifications, (d) faceted hexagonal crystal ($t\simeq 4500$ h, $\rho\simeq 0.1$, $v_g\simeq 5\times 10^{-6}$ μm/sec) with small seed crystal shown in the left inset.

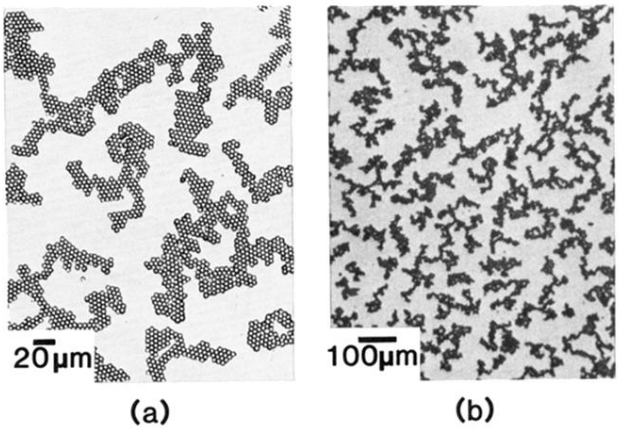

FIG. 3. DLCA of 4.7-μm spheres ($\rho=0.14$) showing (a) crystalline behavior on short length scales and (b) ramified clusters on large length scales.